

# Stability of surface and bulk nanobubbles

Beng Hau Tan<sup>a</sup>, Hongjie An<sup>b</sup>, Claus-Dieter Ohl<sup>c</sup>

<sup>a</sup>*KB Corporation, 7500A Beach Road, 199591 Singapore*

<sup>b</sup>*Queensland Micro and Nanotechnology Centre, Griffith University, 170 Kessels Road, Nathan, Queensland 4111, Australia*

<sup>c</sup>*Otto von Guericke University Magdeburg, Department for Soft Matter, Institute for Physics, Universitätsplatz 2, 39106 Magdeburg, Germany*

---

## Abstract

The existence of stable nanoscopic gaseous domains in liquids, or nanobubbles, has attracted both scepticism and intrigue, since classical theory predicts that spherical gas bubbles cannot achieve stable equilibrium. Can we prove these gaseous domains exist, and if they do, how do they survive? We critically review contemporary theoretical perspectives of the stability of surface and bulk nanobubbles, and explain how experiments either vindicate or disprove them. We then conclude with a discussion of unanswered questions and propose future directions for the field at large.

---

## 1. Introduction

A bubble is a spherical void in a continuum of liquid—a system that occurs everywhere in nature and industry where gases interact with liquids. Bubbles exhibit a bewildering range of behaviours over ten orders of magnitude in space and time, the result of a confluence of multiple effects—capillarity, viscosity, inertia, confinement, geometry and diffusive gas transport among them. While cavitation bubbles predominantly containing vapour lead short ( $\sim \mu\text{s}$ ) and violent lives, emitting shockwaves and even light as they evolve [1], bubbles of atmospheric gas attached to the walls of a glass of cold water are long-living. A sufficiently large and untethered bubble, however, will rise through the containing liquid by buoyancy (see Fig. 1(a)) and pop as a fast liquid jet as the liquid-gas interfaces of the bubble and the liquid pool meet [2].

---

*Email addresses:* bhi.tan@gmail.com (Beng Hau Tan), hongjie.an@griffith.edu.au (Hongjie An), claus-dieter.ohl@ovgu.de (Claus-Dieter Ohl)

The last two decades have seen substantial academic and industrial interest in bubbles of nanoscopic dimensions. Such *nanobubbles* are expected to exist in two forms: either attached onto surfaces (‘surface nanobubbles’) or freely suspended spherical bubbles (‘bulk nanobubbles’), see Fig. 1(b). Industrial interest originates from the idea that dynamically stable and small bubbles will avoid the typical demise by buoyancy, allowing them to intervene in applications ranging from water treatment, lake remediation, fabrication of foams, cleaning of fouled surfaces, to the treatment of diseases [3]. The objects known also as ‘ultrafine bubbles’ are at the centre of a burgeoning industry valued by the Wall Street Journal at US\$10 billion in 2020 [4].

Considering the maturity of the industry around nanobubbles, it may come as a surprise that the academic intrigue over nanobubbles is about whether they even exist, and if so, how they manage to survive. A broad corpus of experiments over the last 20 years stands at odds with the widely accepted classical prediction that spherical bubbles are unstable to diffusion under standard conditions. Growing calls to deploy nanobubbles in ambitious but risky frontiers such as human medicine make it necessary to bridge the yawning gap between industrialization and fundamental understanding as quickly as possible.

The aim of this paper is to critically survey recent theoretical developments about surface and bulk nanobubbles. This paper focuses on the historical problem of nanobubbles containing atmospheric gases, and largely neglects emergent systems of nanobubbles that are produced under extreme conditions such as boiling or electrochemistry. Our review discusses stability theories for surface nanobubbles and bulk nanobubbles, and novel recent insights from computational studies, as well as a critical perspective about the advantages and limitations of some of these contemporary viewpoints. We conclude with an outlook of future directions and open problems.

## 2. Why can’t a spherical bubble survive?

The scientific intrigue over nanobubbles originates from the classical expectation that nanobubbles should not survive. Consider a spherical bubble that predominantly contains atmospheric gases (as opposed to a vapour bubble), and which is present in an infinite volume of liquid; we neglect buoyancy at the moment. One of the most celebrated theories in fluid dynamics is that, being a permeable interface, the transport of dissolved gas between the bubble and the surrounding liquid obeys the diffusion equation  $c_t = D\nabla^2 c$ , where  $D$  is the diffusion constant,  $t$  is time (the subscript denotes a derivative),  $\nabla^2$  is the Laplace operator

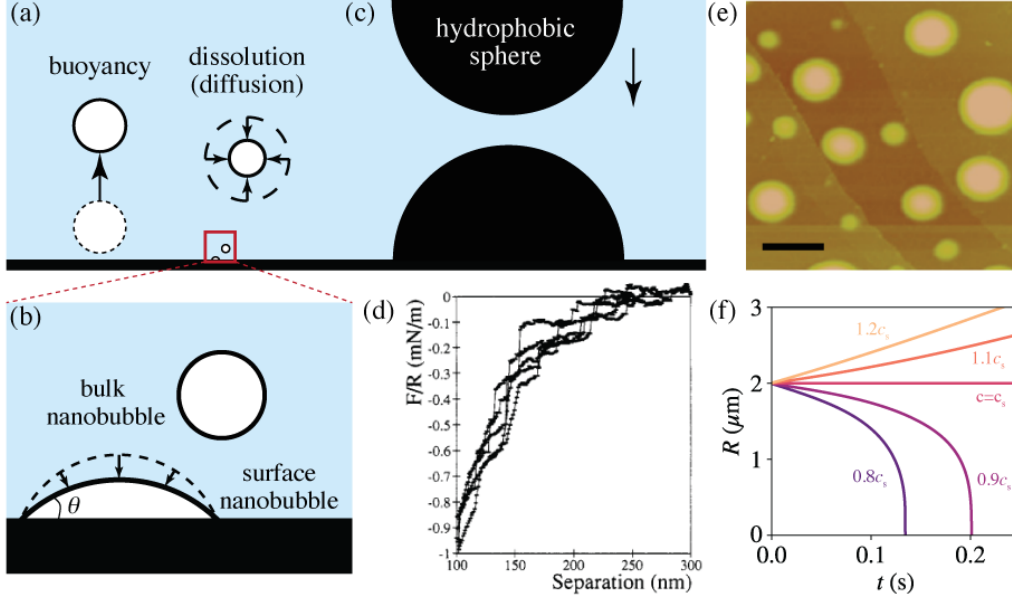


Figure 1: (a) The fates of a bubble: a macroscopic ( $\gg \mu\text{m}$ ) bubble will rise up the liquid until it meets the top of the liquid-gas surface, or dissolves by diffusive transport. (b) Schematic representations of a surface and a bulk nanobubble. (c) The ‘origin story’ of surface nanobubbles. SFA experiments [5] resolve the interaction force between immersed hydrophobic spheres. (d) Parker *et al.* [5] attributed discrete steps in the interaction force between immersed hydrophobic spheres to surface nanobubbles. (e) Image of surface nanobubbles as seen in tapping mode AFM, from Teshima *et al.* [6]. (f) The ‘Laplace pressure bubble catastrophe’ [3]. The dynamics of bubble radii  $R(t)$  as the gas concentration in the liquid is adjusted from below saturation  $c < c_s$ , to above saturation  $c > c_s$ . In the former case, a bubble will dissolve into bulk liquid, and in the latter it will grow without bound. The point  $c = c_s$  is an unstable equilibrium, and in practical situations, perturbations in solubility (e.g. from temperature variations) will steer the bubble towards one or the other aforementioned outcomes.

49 and  $c$  is the concentration field. Using a well-known exact solution [7], Epstein  
 50 and Plesset [8] suggested that the dynamic equation of a spherical bubble obeys

$$\frac{dR}{dt} = -\frac{D}{\rho_g} \left( \frac{P_0}{k_H} + \frac{2\gamma}{k_H R} - c_\infty \right) \left( \frac{1}{R} + \frac{1}{\sqrt{\pi D t}} \right), \quad (1)$$

51 where  $\rho_g$  is the density of gas and  $\gamma$  is the surface tension. The conversion between  
 52  $c$  and  $R$  is facilitated by Henry’s law, which states that the dissolved gas concen-  
 53 tration in the liquid phase adjacent to the bubble is proportional to the internal  
 54 pressure  $P$  in the gas phase of the bubble.

55 One consequence of the Epstein-Plesset equation is that all spherical gas bub-

bles are diffusively *unstable* in practical situations. We can prove this by directly solving Eq. (1) across a range of dissolved gas concentrations  $c_\infty$ , with respect to its saturation concentration  $c_s = (2\gamma/R + P_0)/k_H$ , where  $k_H$  is the Henry constant, see Fig. 1(f). In an undersaturated liquid  $c_\infty < c_s$ , the bubble shrinks until it dissolves completely; this process is accelerative since the Laplace pressure  $P_0 + 2\gamma/R$  driving the shrinkage diverges as  $R$  decreases. In oversaturated liquid  $c > c_s$ , reciprocal arguments apply, but in practice the main cause for demise is that the bubble rises out of the liquid once work done on it by buoyancy  $\sim \rho R^4 g$  exceeds the thermal energy  $\sim k_B T$ . (Balancing these terms yields  $R \approx \sqrt[4]{k_B T / \rho g} \sim 1 \mu\text{m}$ .) This leaves the final possibility,  $c_\infty = c_s$ . Although a first glance of Eq. (1) suggests the bubble stabilizes here, explicit solution reveals that the point is an unstable equilibrium. Any transient gradients of temperature and solubility would therefore nudge the bubble into either unbounded growth or dissolution. We should also note that these theoretical predictions are upheld by experimental validation, down to the resolution limits of the experimental techniques used. A long distance microscope can resolve bubble sizes as small as  $R \approx 5 \mu\text{m}$  [9], while careful resistive pulse experiments by Berge [10] probe bubble radii as small as  $R \approx 1.5 \mu\text{m}$ .

### 3. Surface nanobubbles

The story of surface nanobubbles has its roots not in fluid dynamics, but in the development of a liquid-medium surface force apparatus (SFA) by Jacob Israelachvili, which heralded a generation of study in fundamental interactions between liquid-immersed surfaces (see Fig. 1(c) and Ref. [11]). SFA measurements predict the existence of a ‘short-ranged hydrophobic interaction’ with a range of about a nanometer, which is found to be attractive or repulsive depending on the choice of spheres and the intervening liquid. In 1994, Parker, Claesson and Attard [5] reported a ‘long-ranged interaction’ at the  $\sim 100 \text{ nm}$  length scale. Unlike the interaction curve at the  $\sim 1 \text{ nm}$  range, which varies continuously, the long-ranged interaction was unexpectedly discrete, presenting random (but not quantized) jumps (see Fig. 1(d)). Parker, Claesson and Attard attributed the jumps to gaseous ‘nanobubbles’. A new field of soft matter was born.

The postulated existence of surface nanobubbles immediately invited scepticism on both experimental and theoretical grounds. Experimental objections centred around the inability to reproduce the findings by Parker, Claesson and Attard [5]; some neutron scattering experiments did not reproduce their key assumption that bubbles are entrained on water immersed hydrophobic surfaces [12, 13].

The theoretical objections centred around the categorical prediction by Epstein and Plesset that spherical bubbles should dissolve within  $\sim 1 \mu\text{s}$  of nucleation.

Theoretical objections notwithstanding, experiments—particularly tapping mode atomic force microscopy [14, 15, 16, 17, 6], see Fig. 1(e)—over the last two decades have confirmed the presence of stable, flat, spherically capped surface nanobubbles on liquid-immersed surfaces (often, but not always hydrophobic) with heights  $h \sim 10 - 100 \text{ nm}$  and footprint radii  $L \sim 100 - 1000 \text{ nm}$ . The experimental objections were addressed by the eventual realization that surface nanobubbles do not always spontaneously nucleate on immersed surfaces, but specific nucleation techniques (which compel nucleation by increasing local gas oversaturation) will quite reproducibly produce nanobubbles on demand. The field has also had to overcome a widespread issue with contamination, which we discuss in detail in a companion paper.

In short, experiments reveal that surface nanobubbles possess the following properties:

1. Surface nanobubbles survive for as long as researchers have bothered to wait, which in this case is about four weeks.
2. Their contact angles are small as measured from the gas phase, regardless of the combination of liquid or substrate, and typically range from  $5-20^\circ$ . Curiously, the angles are unrelated to the Young contact angle measured at the macroscale.
3. They are stable in some types of liquids, notably water, but then dissolve when immersed in some organic solvents, such as ethanol [18, 19].
4. In water, surface nanobubbles are often found on hydrophobic surfaces such as silanized silicon wafer, but also on hydrophilic substrates such as highly ordered pyrolytic graphite (HOPG), or even glass.
5. Upon a change to the dissolved gas concentration  $c_\infty$  in the liquid, the bubbles grow or shrink into a new height over several hours [15].
6. When dissolved gas is removed from the liquid, surface nanobubbles shrink but remain stable [14, 15]. Surface nanobubbles survive the removal of as much as 80% of the dissolved gas in the bulk liquid [20]. This is remarkable because the Epstein-Plesset theory predicts that spherical gas bubbles dissolve immediately once the dissolved gas concentration falls below exact saturation.

In the rest of this section we outline the major theoretical milestones in arriving at a theory of stability for surface nanobubbles that is capable of explaining all of these major properties.

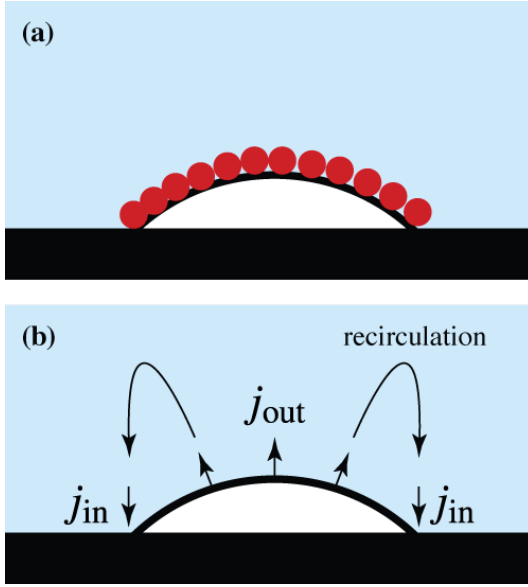


Figure 2: (a) The contaminant barrier hypothesis supposes that surface nanobubbles are coated in a layer of organic contamination that renders them entirely impermeable to gas. (b) The dynamic equilibrium model [21] assumes that gas outflux  $j_{out}$  is compensated by an influx near the substrate,  $j_{in}$ . Continuity implies the existence of a large-scale recirculation flow with typical velocity 1 m/s [22], though experiments subsequently failed to find evidence of such flows [18, 23].

### 129 3.1. Local transport: hydrophobicity and dynamic equilibrium

130 The earliest attempts to rationalize the existence of surface nanobubbles fo-  
 131 cused on transport of gas in the immediate vicinity of the bubble. One potentially  
 132 trivial explanation for stability is that the bubble is simply impermeable to gas,  
 133 such as by a covering of contamination [24], see Fig. 2(a). However, experiments  
 134 disproved this hypothesis by showing that surface nanobubbles do respond to envi-  
 135 ronmental changes in dissolved gas concentration (**Property 5**) and are therefore  
 136 gas permeable [14, 25].

137 A second major avenue was inspired by the finding in early experiments that  
 138 nanobubbles nucleate on hydrophobic surfaces. Such hydrophobic surfaces attract  
 139 gas in preference to water, with the consequence that the dissolved gas concen-  
 140 tration within about 1 nm from the substrate, where short-ranged attraction is  
 141 dominant, should be higher than in the bulk liquid, where the attraction dimin-  
 142 ishes [26]. Brenner and Lohse [21] argued that this reservoir of gas enrichment  
 143 should contribute an influx of gas at the nanobubble's three phase line that should  
 144 exactly cancel out gas outflux from the bubble, which was assumed constant over

145 the bubble (see Fig. 2(b)). However, what was known as the *dynamic equilibrium*  
 146 model suffered from the conceptual difficulty that a convective current would be  
 147 required to connect the outflux to the influx. Such a convection would not only  
 148 require an external source of energy but even implies that a nanobubble should  
 149 emit a strong liquid jet with a velocity of 1 m/s [22]. In any case, the dynamic  
 150 equilibrium model fell out of favour after experiments from separate groups found  
 151 that tracer particles seeded in the vicinity of surface nanobubbles exhibit dynamics  
 152 indistinguishable from Brownian motion [18, 23].

### 153 3.2. Global transport: the traffic jam model

154 Instead of contending with gas transport local to a surface nanobubble, Weijs  
 155 and Lohse [27] instead consider the much broader problem of gas transport *through-*  
 156 *out* the entire liquid that hosts the surface nanobubbles. They consider a semi-  
 157 infinite, one dimensional system with a surface nanobubble at one side and the  
 158 top of a liquid pool on the other, see Fig. 3(a). Since the nanobubble's internal  
 159 pressure is  $P_0 + 2\gamma/R$  and unconditionally larger than the saturation concentration  
 160 of the liquid, it serves as a source of gas oversaturation, losing its excess dis-  
 161 solved gas to the ambient environment over time. Consequently the Weijs-Lohse  
 162 model explains for the first time the remarkably slow dynamic response of sur-  
 163 face nanobubbles to environmental stimuli (**Property 5**): the liquid's thickness  $\ell$   
 164 establishes its diffusion timescale  $\tau \sim \ell^2/D$ , extending to 10 hours when  $\ell \sim 1$   
 165 cm. However, it incorrectly predicts surface nanobubbles would shrink gradually  
 166 until they dissolve. Instead, experiments show that on a change of the liquid's  
 167 dissolved gas concentration, surface nanobubbles reach a new equilibrium height  
 168 after several hours (**Properties 1 and 5**). The model also conspicuously neglects  
 169 the influence of either the liquid or the substrate (**Properties 3 and 4**).

### 170 3.3. Contact line pinning and oversaturation

171 In parallel to the aforementioned early ideas on local and global transport, lat-  
 172 tice density functional theory calculations by Liu and Zhang [28, 29, 30] identified  
 173 two other potential sources of stability. Experiments show that surface nanobub-  
 174 bles observe *contact line pinning*, maintaining a constant footprint even as they  
 175 grow or shrink in height. The Liu-Zhang simulations showed that a line-pinned  
 176 (imposed by either chemical or physical defects) surface nanobubble in a liquid  
 177 that is oversaturated with dissolved gas achieves thermodynamic metastability.

178 An elegant mechanistic insight for the unexpected stability was subsequently  
 179 supplied by Lohse and Zhang [31] and by Chan, Arora and Ohl [32]. Both ap-  
 180 proaches start from the realization that the unstable equilibrium experienced by a

shrinking spherical bubble is ultimately driven by its geometry. They reparameterise the dynamic equation in the Epstein-Plesset model from a spherical bubble of radius  $R$  to that of a line-pinned *spherical capped* surface nanobubble through elementary geometric identities. These theories implement contact line pinning by setting the footprint radius  $L$  constant, leading to a dynamical equation either as a function of height  $h(t)$  or contact angle  $\theta(t)$ . With the reparameterisation, surface nanobubbles achieve stable equilibrium when [31]

$$\zeta = \frac{2\gamma}{LP_0} \sin \theta_e. \quad (2)$$

Without contact line pinning, a spherical cap bubble would be able to grow or shrink proportionally, and in that case would also experience the same unstable equilibrium experienced by freely suspended spherical bubbles.

The pinning-oversaturation model takes a key step in overcoming the conceptual difficulty in understanding why bubbles should not immediately dissolve (see Section 2). However, it also raises fresh conceptual difficulties of its own. First, it was quickly pointed out [33] that Eq. (2) requires  $\zeta > 0$  for a non-zero contact angle, meaning that the pinning-oversaturation model cannot explain how surface nanobubbles can exist at ambient conditions ( $\zeta = 0$ , see **Property 1**), or when the liquid is degassed ( $\zeta < 0$ , see **Property 6**). Second, the model implies that the bulk liquid cannot be in thermodynamic equilibrium, since it is required to hold dissolved gas beyond saturation. Third, the model does not natively explain how stability is affected by the liquid and substrate (**Properties 3 and 4**).

### 3.4. Tying loose ends together: the TAO model

The three aforementioned models—dynamic equilibrium, traffic jam and pinning-oversaturation—pursue very different perspectives of stability and are thus not mutually exclusive. A pair of papers by Tan, An and Ohl [34, 35] argue that these ideas—when suitably modified—can be unified within a single framework.

The key issue with the pinning-oversaturation model was that the indefinite stability of a surface nanobubble is contingent on the presence of permanent gas oversaturation in the bulk liquid; this assumption is unrealistic because at thermodynamic equilibrium the bulk liquid must be exactly saturated (i.e.  $\zeta = 0$ ). However, the framework of Brenner and Lohse [21] offers a solution to this conundrum: the solid substrate is not an inert boundary but attracts dissolved gas locally. Crucially, this local gas enrichment persists at thermodynamic equilibrium and constitutes the source of *permanent* oversaturation that was sought after



214 in the pinning-oversaturation model. By generalising the Lohse-Zhang condition  
 215 [Eq. (2)], Tan, An and Ohl [35] yield the revised stability condition

$$\int_0^h \left( \frac{2\gamma}{LP_0} \sin \theta_e - \zeta(z) \right) dz = 0, \quad (3)$$

216 whose root yields the equilibrium contact angle  $\theta_e$  under the influence of the po-  
 217 tential  $\phi$ . The TAO model maintains the stable equilibrium that is predicted by  
 218 the pinning-oversaturation model. It is especially noteworthy that the geometry of  
 219 the surface nanobubble enforces the equilibrium. A disproportionate portion of a  
 220 spherical cap’s surface area is concentrated at its footprint, and even more so as  
 221 the bubble flattens (i.e. its contact angle decreases). Therefore, as a pinned sur-  
 222 face nanobubble shrinks, an increasing proportion of its overall surface area falls  
 223 within the gas enrichment zone, nudging the system towards a state that is already  
 224 known to reach stable equilibrium (see section 3.3). Gas influx occurs at parts of  
 225 the bubble within the interaction distance of the potential  $\lambda$  and outflux occurs at  
 226 heights beyond it (see Fig. 3(b)). Transport is entirely local to the liquid-gas in-  
 227 terface, dispensing with the need for the long-ranged recirculating flows that were  
 228 required in the dynamic equilibrium model.

229 At this point, the dynamic response of surface nanobubbles of  $\sim \mu\text{s}$  remains  
 230 orders of magnitude lower than the true experimental timescale (hours). To re-  
 231 solve this remaining shortcoming [35], TAO couple these effects—which are lo-  
 232 cal to the surface nanobubble, see Fig. 3(b)—to the broader problem of global  
 233 transport of dissolved gas through the liquid to the outside world (Fig. 3(a)) as  
 234 first tackled by Weijs and Lohse [27]. Due to a disparity of length (nm vs. m)  
 235 and time ( $\mu\text{s}$  vs. min) scales of the global and local problems, TAO argue that  
 236 the nanobubble’s contact angle can be assumed to respond instantaneously to en-  
 237 vironmental changes in gas concentration in the global problem. Thus, as they  
 238 envisage it, surface nanobubbles gradually adjust to a stable equilibrium angle  
 239 that is jointly determined by both the macroscopic environment (through  $c_\infty$ ) and  
 240 the microscopic affinity  $\phi$  between the gas and the substrate (Fig. 3(c)).

241 The downside of the TAO model, however, is that the effective gas-substrate  
 242 potential  $\phi$  must be known. Their calculations assume an *ad hoc* dependence with  
 243 a typical attractive strength  $\sim k_B T$ , and an interaction distance  $\sim 1$  nm. With  
 244 these assumptions, most of the key experimental properties are explainable: sur-  
 245 face nanobubbles reach a stable equilibrium (**Property 1**) at small contact angles  
 246 (**Property 2**); respond to changes in dynamic stimuli slowly; (**Property 5**), and  
 247 survive even when the liquid is strongly degassed (**Property 6**).

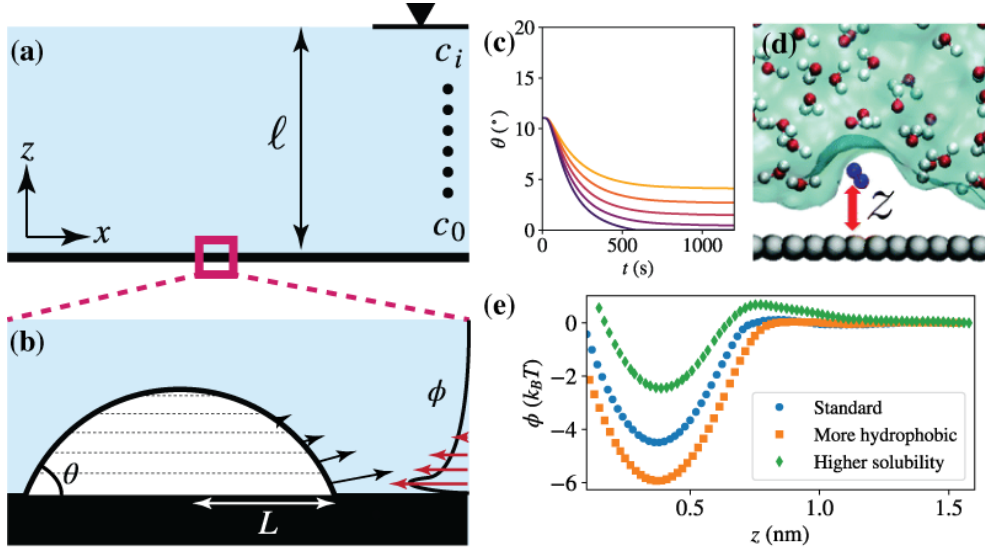


Figure 3: The interplay of liquid, gas and solid interactions affects the stability of surface nanobubbles. (a-b) The TAO model [34, 35] connects global transport effects (Ref. [27] and Fig. 2(b)) with a local gas enrichment facilitated by an effective attraction. (c) Gas enrichment implies that surface nanobubbles can survive degassing of the liquid. The curves from top to bottom (which use an ad hoc potential [35]) show a system in which 0%, 25%, 50%, 75% and 100% of the dissolved gas in the bulk liquid is removed; the nanobubble here survives 75% degassing. (d-e) The potential of mean force  $\phi(z)$  between a nitrogen molecule and a water-immersed graphene substrate. The interaction for standard values is highly attractive ( $-4.5k_B T$ , blue circles). On a more hydrophobic surface (weaker liquid-gas interaction), the effective gas-solid attraction is stronger (orange squares). In contrast, the attraction is significantly weakened in a liquid of  $5\times$  the gas solubility of water (by defining stronger liquid gas interaction; green diamonds).

### 248 3.5. The potential of mean force

249 Despite its successes, the TAO model is not by itself a complete framework  
 250 for the stability of surface nanobubbles. It does not—directly at least—address at  
 251 least two remaining key properties: how stability is affected by the identities of  
 252 the liquid and the substrate (**Properties 3 and 4**). Rather, it reframes the ques-  
 253 tion “what stabilizes a surface nanobubble?” into “what is the effective potential  
 254 between the gas and the substrate?”

255 The *potential of mean force* (PMF) between the nitrogen and the liquid-immersed  
 256 substrate convolves a multitude of disparate intrinsic mutual interactions between  
 257 the gas molecule and the liquid-immersed substrate mediated by the molecular  
 258 structure of the liquid (Fig. 3(d)). Although it can neither be experimentally nor  
 259 theoretically derived, the PMF can be calculated by rare event sampling molecu-

lar dynamics, as shown by Tortora *et al.* [36]. Their calculations, see Fig. 3(e), indicate that the PMF is attractive ( $\sim k_B T$ ) over 1 nm, consistent with the assumptions of Tan, An and Ohl [34]. When the calculated  $\phi(z)$  is used in the TAO model, one recovers equilibrium contact angles in the range of 5-20°, in strikingly good agreement with experiments [37, 17], though we urge caution in making direct comparisons between experiments and MD simulations (see Section 3.6).

By varying the balance of interactions between gas, solid and liquid, the PMF calculations of Tortora *et al.* [36] provide a singularly unique perspective about how macroscopically accessible quantities like wettability and gas solubility influence the stability of surface nanobubbles. To simulate a more hydrophobic surface, they use a weaker liquid-solid interaction, which leads to a deepened attraction (orange squares, Fig. 3(e)); note that the enhanced interaction arises without modifying the interaction with the dissolved gas. In contrast, a liquid with approximately  $5\times$  the gas solubility of water, implemented by increasing the liquid-gas interaction, diminishes the attraction considerably (green diamonds, Fig. 3(e)). The reason why we describe these findings as “unique” is that they show how the liquid plays a decisive role in determining stability, even though *all* the models discussed so far conspicuously regard the liquid as a purely inert medium. These calculations therefore offer straightforward explanations for observation that surface nanobubbles can exist on both hydrophilic and hydrophobic surfaces (**Property 4**), and for their instability in organic solvents, such as ethanol (**Property 3**). These insights, along with the properties explained by the TAO model, lead to the simultaneous explanation of all six of the major experimental properties of surface nanobubbles.

### 3.6. Novel perspectives: adsorption effects

In parallel, several novel perspectives have also emerged in recent years. One emerging class of models suggest that strong adsorption of gas molecules to the substrate. It should be noted that adsorption effects do not necessarily contradict the ideas presented in previous sections, but their presence can lead to interesting or counterintuitive effects.

Petsev, Leal and Shell [38] argue that some portion of the gas molecules inside the nanobubble are chemisorbed to the surface, and with fewer ‘free’ gas molecules in the gas phase, a surface nanobubble would have a lower internal pressure and adopt a flatter shape (**Property 2**). However, the authors make the assumption that materials used in surface nanobubble experiments such as HOPG have comparable adsorption constants to metal organic frameworks and other materials specially functionalized for gas capture. Given that the adsorption constant

is exponentially dependent on adsorption enthalpy [39], these calculations may significantly overestimate the effect of adsorption on the bubble shape. Maheshwari *et al.* [40] have also suggested that gas molecules from one surface nanobubble are strongly attracted (or physisorbed) to the planar substrate, translating along it along a ‘gas tunnel’, before reaching a neighbouring nanobubble. If the interaction parameters do correspond to a physically occurring system, these ‘gas tunnels’ may allow surface nanobubbles a novel path to Ostwald ripen or coalesce, effects that are theoretically forbidden by contact line pinning [41].

One of the most radical theoretical ideas about surface nanobubbles is the claim that surface nanobubbles are not gaseous at all, but are quasi-liquid condensates with a density comparable to liquid nitrogen, even at room temperature and pressure [42]. If they exist, ultradense condensates would be of monumental importance to society, since the transportation and handling of dilute gases is the single biggest technological bottleneck to the widespread adoption of clean hydrogen technologies. It should be pointed out that claims of ultradense bubbles in MD simulations have a history stretching up to 15 years [43, 44, 45], but has come into renewed focus recently due to experiments that claim *quantitative* agreement with the MD simulations [42, 46]. However, the mechanistic details of the quasi-liquid condensate hypothesis need to be carefully resolved. One can understand that gas might be present at higher densities within the 1 nm interaction distance of the PMF (see Fig. 3(e)), but this leaves open the question of what is holding gas molecules to the tune of  $200\times$  the density of an ideal gas beyond the interaction distance, where the gas-substrate PMF is zero.

These examples reflect the hazards of drawing literal inspiration from molecular dynamics simulations. It is frequently overlooked that MD studies currently do not simulate realistically gas-solvated liquids. Nitrogen dissolves in liquid at a mole fraction of  $10^{-5}$  [47], implying that a bubble containing just 10-100 gas molecules would require system sizes of  $10^6 - 10^7$  molecules, out of the reach of most computational research groups today. Consequently, *all* MD studies that we are aware of suffer from the common flaw of using unrealistically high mole fractions of  $10^{-3} - 10^{-2}$ , that is, hundreds to thousands of times beyond their true saturation concentration. In our view, the ultrahigh densities reported across more than a decade’s worth of MD simulations [43, 45, 48, 42] may well be an artifact of the extreme oversaturations unique to MD. Moreover, MD studies typically deploy periodic boundary conditions that prevent the excess oversaturation from exiting the computational domain. Thus, gas molecules in an MD system exist in an frustrated metastable state in which gas molecules are left with no other recourse but to accumulate at high density within the nanobubble.

335 3.7. *Novel perspectives: is contact line pinning necessary for stability?*

336 A recent fluorescence microscopy study by Bull *et al.* [49] suggests that sur-  
337 face nanobubbles can survive without contact line pinning, invalidating the theo-  
338 retical foundations established by the pinning-oversaturation model (see Section  
339 3.3). By repeatedly cycling ethanol and water over a substrate, they observe that  
340 surface nanobubbles nucleate on the same locations on glass, but on a copoly-  
341 mer brush, the nucleation sites are not reproducible. Unlike the glass, the authors  
342 suggest that the polymer brush continuously reconfigures as it absorbs solvent,  
343 smoothing out physical defects that they presume contribute to contact line pin-  
344 ning. However, reconfiguration of the mobile tails of the copolymer brush also  
345 means that the chemical heterogeneity landscape of the surface will also dynam-  
346 ically change; thus the irreproducible nucleation on copolymer brushes has a po-  
347 tentially trivial explanation unrelated to line pinning. Further, the authors appear  
348 to have the fundamental misconception that only physical defects contribute to  
349 contact line pinning, leading them to neglect at least two other sources of contact  
350 line pinning in their experiments. Contact lines can be immobilized on atomically  
351 flat surfaces if the surface contains chemical heterogeneities [50, 51], or if the sub-  
352 strate is sufficiently soft, in which case pinning is triggered [52, 53] through an  
353 out-of-plane elastocapillary force [54]. Follow up claims that surface nanobubbles  
354 are stable without contact line pinning should therefore control for at least three  
355 sources of contact line pinning: physical heterogeneity, chemical heterogeneity  
356 and softness.

357 **4. Bulk nanobubbles**

358 Much like surface nanobubbles, the story of bulk nanobubbles started as a the-  
359oretical construct, tracing back to approximately the middle of the last century.  
360 Theoretical considerations predict that pure water needs to be stretched by a ten-  
361sile stress in the order of a thousand atmospheres before the onset of cavitation.  
362 However, experiments *universally* find that bubbles spontaneously form in water  
363 at vastly smaller tensile stresses, even when special effort is taken to ensure the  
364 purity of the water. The most persistently presented explanation for the dramatic  
365 reduction of tensile stress of water is that the liquid contains compressible pockets  
366 of *cavitation nuclei* [55], which would respond more readily to stress variations  
367 than the pristine liquid. Such nuclei can be entrained in crevices in vessels bearing  
368 liquid, present on flat immersed surfaces (i.e. surface nanobubbles), or suspended  
369 in the bulk liquid (bulk nanobubbles).

370 The difficulty, however, is in experimental validation of this theoretical con-  
371 struct. There are a wide variety of techniques to characterise surface nanobubbles  
372 that are fixed onto surfaces, and perhaps more importantly, experimental tech-  
373 niques that corroborate that the objects are gaseous. In the case of bulk nanobub-  
374 bles there is no shortage of methods that claim to be able to produce them; un-  
375 fortunately there is no experimental technique that is able to authoritatively prove  
376 that the objects produced are actually gaseous.

377 Bulk nanobubbles are predominantly characterized by dynamic light scatter-  
378 ing (DLS). In short, a coherent light source such as a laser is directed into the  
379 liquid, creating a speckle as light scatters off suspended objects. One or more  
380 photodetectors that are aligned oblique to the illumination axis measure the tem-  
381 poral persistence of the resulting speckle, recovering a histogram of particle sizes.  
382 Although it is widely used, DLS cannot distinguish among bubbles, droplets or  
383 particles, a fatal limitation in a field that has a long history of irreproducible re-  
384 sults and contaminated results. DLS results can drastically change if liquids are  
385 redistilled [56] or, even more alarmingly, DLS spectra attributed to nanobubbles  
386 can disappear when care is taken to clean experimental vessels [57].

387 Having prefaced with the caveat that DLS experiments are not definitive, we  
388 briefly outline the properties that DLS attribute to bulk nanobubbles:

- 389 1. Bulk nanobubbles have an implied radius  $\sim 100$  nm.
- 390 2. The implied radii of bulk nanobubbles has a maximum of several hundred  
391 nanometers, generally well below the  $1\ \mu\text{m}$  limit beyond which buoyancy  
392 dominates and the bubble will rise out of the liquid.
- 393 3. The implied radii of bulk nanobubbles is responsive to ionic chemical ad-  
394 ditives; although there is considerable scatter in experiments between in-  
395 dividual groups, there is consensus that the bubble radius increases with a  
396 decrease in a liquid's Debye length.

397 In the last few years, the experimental literature has fissured into two camps.  
398 One camp unequivocally proclaims to have adduced undisputable evidence for the  
399 existence of bulk nanobubbles in pure water [58, 59]. The other is adamant that  
400 the experiments clearly rule out that bulk nanobubbles can exist in pure water, and  
401 that such objects can likely only exist when armoured with particles or some other  
402 coating [60, 61, 62]. The ongoing debate has occasionally taken an ugly turn, with  
403 one group describing sceptics of bulk nanobubbles as basing their conclusions on  
404 “either questionable experimentation or sheer speculation” [58].

405 This section will critically discuss the major proposed stability mechanisms  
406 for the existence or stability bulk nanobubbles and explain the degree to which

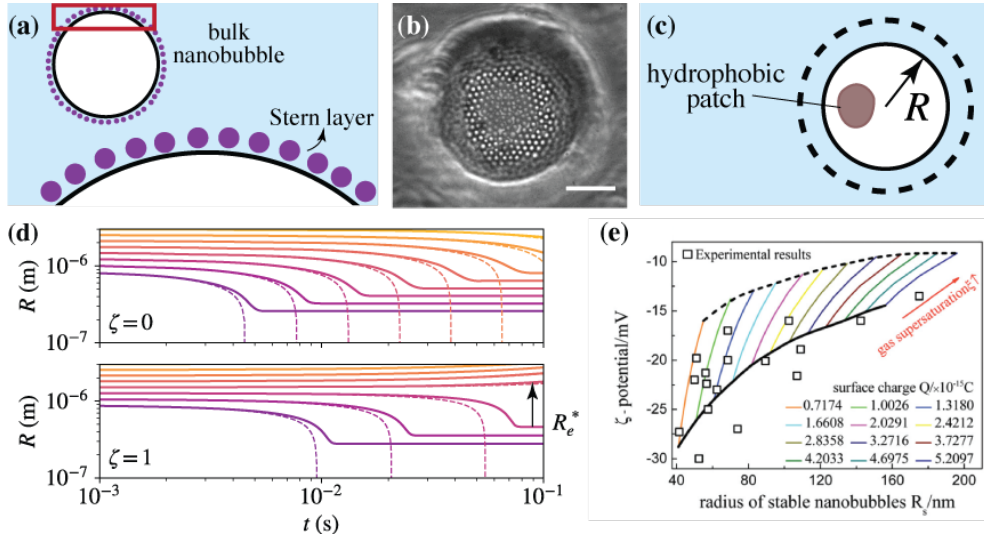


Figure 4: Contemporary perspectives of the stability of bulk nanobubbles. (a) Akulichev’s model [63] proposes that, given experimental reports that bubbles are negatively charged, a diffuse electric double layer (here only the Stern layer is shown) assembles at the liquid-gas interface, whose electrostatic stress balances with the bubble’s Laplace pressure. (b) A microbubble stabilized by an armour of particles. As the bubble shrinks, the particles jam together more strongly, therefore reinforcing mechanical stability. Scale bar, 30  $\mu\text{m}$ . (c) Yasui’s model [64] proposes that a bulk nanobubble is stabilized by a hydrophobic, gas permeable patch that experiences gas influx, balancing exactly with outflux from pristine regions of the bubble. (d-e) The models of Tan-An-Ohl [65] and Zhang-Guo-Zhang [66] extend the Akulichev model consider the gas oversaturation in the liquid; they find that oversaturation establishes a maximum size that a nanobubble can achieve. Moreover, the TAO model predicts that spherical bubbles will follow Epstein-Plesset dynamics before abruptly stabilizing at a few hundred nanometer radius.

407 recent experiments support or disprove them. In short, our position is that as a  
 408 matter of physical principle, bulk nanobubbles can exist, but neither camp in the  
 409 ongoing debate among experimentalists has authoritatively proven or disproven  
 410 the existence of bulk nanobubbles.

#### 411 4.1. Akulichev’s model: stabilization by surface charges

412 It has been known since the late 19th century [67, 68] that a bubble in neutral  
 413 pH liquid carries an electrical charge. When released between electrodes of op-  
 414 posing polarity, the bubble migrates towards the cathode. As far as we are aware,  
 415 the first to link this property to the possible stability of a spherical bubble was V.  
 416 Akulichev [63]. All models of bulk nanobubble stabilization by surface charges  
 417 essentially rely on this single insight, with perhaps the most consistent proponent

418 of the idea in recent years being the group of Bunkin [69], who refer to these  
419 objects as “bubbstons”.

420 In short, the charge stabilization model assumes that the surface charge den-  
421 sity  $\sigma$  on the bubble creates an electrostatic pressure  $P_e = \sigma^2/2\epsilon_r\epsilon_0$ , where  $\epsilon_0$  is  
422 the permittivity of free space and  $\epsilon$  is the relative permittivity of water. Akulichev  
423 made the key insight that  $P_e$  acts *opposite* to the Laplace pressure  $P = P_0 + 2\gamma/R$ .  
424 The tensile nature of surface tension means that at every point on the curved sur-  
425 face of the bubble, components of force tangential to the surface cancel out ev-  
426 erywhere, leaving a component directed towards the bubble’s centre. However,  
427  $P_e$  acts in the opposite direction: surface charges mutually repel, and by similar  
428 symmetry arguments produces a force that acts radially outward—that is, oppo-  
429 site to the Laplace pressure. It is therefore expected that the two contributions  
430 cancel when  $P(R_e) = P_e(R_e)$ , leading to an equilibrium when the bubble’s radius  
431 is  $R = R_e$ . This equilibrium can be shown to be a stable one [65, 66], avoiding the  
432 conceptual issue that afflicted surface nanobubbles for years.

433 This formulation invites the question of how to provide a quantitative measure  
434 of the charge density. A charged interface should lead to the assembly of dissolved  
435 ions in an electric double layer around it, and through the Poisson-Boltzmann  
436 equation one obtains, for a bubble of radius  $R$ ,

$$\sigma(R) = \frac{2\epsilon_0\epsilon_r\kappa k_B T}{e} \sinh\left(\frac{e\psi}{2k_B T}\right) f(R). \quad (4)$$

437 Here, the zeta potential  $\psi$  is the electric potential at the distance from the bubble  
438 that delineates mobile bulk liquid from immobile liquid at the double layer, and  
439  $f(R)$  is a correction term that accounts for the curvature of the double layer, de-  
440 rived by Ohshima, Healy and White [70]. Zeta potential measurements generally  
441 find that the potential is negative and is of the order of tens of mV, consistent with  
442 a stable radius in the region of 100 nm [66].

443 One limitation of the classical Akulichev formulation is that it fails to con-  
444 sider the gas oversaturation of the ambient liquid. In the Epstein-Plesset model,  
445 gas oversaturation manifests explicitly in Eq. (1) as a perturbation to the mechan-  
446 ical stress balance. Most protocols that purport to produce bulk nanobubbles tend  
447 to produce clouds or suspensions of bubbles, typically by intense mechanical aer-  
448 ation of the liquid [3]. Since all bubbles have an internal pressure  $P_0 + 2\gamma/R$  ex-  
449 ceeding atmospheric pressure  $P_0$ , the liquid immediately surrounding them must  
450 be gas oversaturated, per Henry’s law. Indeed, measurements with commercial  
451 dissolved oxygen meters suggest that water processed by commercial ‘nanobub-



ble generators' have 400% the dissolved gas concentration of saturated distilled water [71].

The models of Tan, An and Ohl [65] and Zhang, Guo and Zhang [66] account for the contribution of oversaturation to the mechanical stress balance at the bubble's interface, as shown in Figs. 4(d) and (e). When oversaturation is neglected, the mechanical balance of Laplace and electrostatic pressures is *unbounded*, meaning that there is always a unique equilibrium radius  $R$  from balancing  $P_e$  and  $P_L$ . Both papers report that oversaturation establishes an unconditional maximum equilibrium radius for a bubble in the charge stabilization model. This maximum (of a few hundred nanometers) is observed experimentally in DLS experiments, and the considerable variation of this maximum in the experiments may originate from a lack of quantitative control of gas oversaturation in experiments.

#### 4.2. Stabilization by contamination

A second class of stabilization models is that the bubble is armoured by some kind of contamination, such as a particle coating. Unlike other models, there is no controversy whatsoever that this mechanism will work: particle armoured microbubbles are already widely used as ultrasound contrast agents [72, 61]. As a particle-armoured bubble shrinks, the constituent particles coating the interface jam together, exerting a mechanical stress on the interface that acts against Laplace pressure [73]. Since the jamming effect intensifies with the bubble's tendency to shrink, a particle armoured bubble will reach stable equilibrium. K. Yasui has adapted a variation of this idea specifically for bulk nanobubbles [64]. He posits that a gas-permeable hydrophobic contamination barrier may locally attract high concentrations of dissolved gas, allowing for local gas influx, while the regions that are not coated by the contamination experience the usual Epstein-Plesset outflux; the bubble is in dynamic equilibrium when these contributions balance.

However, it is an open question as to whether bulk nanobubbles are truly stabilized by a particle coating. It would be necessary to identify what sources of contamination can be found in abundance in natural systems, and once these sources are identified, to understand how or why such bubbles would universally stabilize at a radius of several hundred nanometers.

#### 4.3. Other perspectives

Let us also discuss some alternative visions for stabilizing bulk nanobubbles. Proponents of the ultradense bubble theory (see section 3.6) have also proposed that if a bulk nanobubble's internal density were several orders of magnitude

larger— i.e. comparable to liquid nitrogen—the bubble’s lifetime would increase by a few orders of magnitude to about a few seconds [44]. However, an increased density has no effect on the unstable equilibrium of the Epstein-Plesset equation [Eq. (1)], and so bulk nanobubbles cannot be long-lived, even with an ultrahigh density.

Manning has recently floated the idea that bulk nanobubbles are stabilized by virtue of the Tolman effect [74]. It is known that the surface tension of a liquid-gas interface substantially deviates from its planar value at very high curvatures  $1/R$  (or very small radii of curvature  $R$ ), which to leading order is

$$\gamma(R) = \gamma \left( 1 - \frac{2\delta}{R} \right), \quad (5)$$

where  $\delta$  is the Tolman length. Although Manning correctly argues that the point  $R = 2\delta$  is one of stable equilibrium, the overall model has several notable weaknesses. First, he questionably deploys the Tolman length as a fitting parameter. For a 100 nm bulk nanobubble to be stabilized, the model demands that the Tolman length be  $\delta \approx 50$  nm, which is three orders of magnitude higher than the consensus estimate (from both experiments [75] and simulations [76, 77]) of  $\sim 1$  Å. Second, stability by the Tolman effect requires that the bubble’s liquid-gas surface tension is identically *zero*. There do exist multiphase systems with ultralow (2-3 orders than the usual 10 mN/m) surface tension [78], but the demand for an interface with zero interfacial tension invites the existential question of whether a cluster of solute molecules in a solvent matrix can even be considered a bubble if not delineated by an interface of finite surface energy.

#### 4.4. *Do bulk nanobubbles exist?*

We end this section by offering our answers to two controversial questions, informed by what we currently understand from these contemporary developments. First, can bulk nanobubbles exist? And second, if they do, which model is the right one?

In an effort to authoritatively prove the existence of bulk nanobubbles, the group of Barigou have performed as many as eleven different types of experiments [58] to complement the DLS measurements. Much as these strenuous efforts are commendable, we are unpersuaded that they individually or collectively constitute “conclusive proof” that bulk nanobubbles exist, because none of the eleven techniques address the fundamental inability of DLS to distinguish bubbles. To make matters worse, the most convincing experimental efforts to directly

521 probe compressibility of DLS light scatterers have failed to find evidence of com-  
 522 pressible objects. The group of Craig [60] subjected water that has been processed  
 523 through commercial ‘nanobubble generators’—i.e. the backbone of the US\$10  
 524 billion ultrafine bubble industry we alluded to in the *Introduction*—in DLS cu-  
 525 vettes whose liquids are subjected to compressive stresses of up to 10 atm. They  
 526 find that the large stresses fail to perturb the DLS-measured histogram of particle  
 527 sizes.

528 However, we should point out that the compressive stress experiments of Al-  
 529 heshibri and Craig [60] do not disprove the particle armouring or the charge sta-  
 530 bilization models. The reason is that both models predict one-sided stability—  
 531 the stabilization feedback from particle jamming or interfacial charge accelerates  
 532 when the bubble shrinks, but diminishes when the bubble grows. In other words,  
 533 the models predict that the size distributions of bulk nanobubbles would fail to re-  
 534 spond noticeably to compressive stresses, but would be unstable to the application  
 535 of large tensile stresses.

536 In our view, the study that comes the closest to proving the existence of bulk  
 537 nanobubbles is a recent set of cleverly designed experiments by Jin *et al.* [79].  
 538 They optically track the shrinkage of microbubbles (whose origin and gaseous  
 539 identity is much easier to ascertain than bulk nanobubbles) with darkfield mi-  
 540 croscopy. The darkfield capability becomes especially important when the ob-  
 541 jects shrink down to (or below) the optical resolution limit of brightfield imaging,  
 542 and using it the authors report that the microbubbles shrink according to Epstein-  
 543 Plesset dynamics before abruptly stabilizing at a few hundred nanometers. No-  
 544 tably, this behaviour is anticipated by the charge stabilization model of Tan, An  
 545 and Ohl [65] (see Fig. 4(d)). At the equilibrium radius, the objects fluctuate with  
 546 Brownian motion, indicating that they are freely suspended in the liquid and not  
 547 attached onto surfaces.

#### 548 4.5. Which model of bulk nanobubble stability is correct?

549 While experiments are yet to authoritatively prove the existence of bulk nanobub-  
 550 bles one way or another, there is nevertheless a large body of experimental results  
 551 from DLS experiments which agree on a few broad points. The charge stabiliza-  
 552 tion model is able to provide reasonable and consistent explanations for the three  
 553 properties claimed by DLS experiments—i.e. its  $\sim 100$  nm radius, the strict max-  
 554 imum limit for the bubble size, and the increase in implied radius as the ionic  
 555 concentration is increased.

556 Although bubbles that are stabilized by contamination barriers indisputably  
 557 exist in some contexts, it is unlikely that this is the mechanism for the stabiliza-

tion of bulk nanobubbles in all cases. Electron microscopy experiments of water claimed to be infused with nanobubbles show *featureless* voids of several hundred nanometers [80], implying that any contamination that is present has to be smaller than the  $\sim 1$  nm spatial resolution of an electron microscope. While the contamination barrier models are mechanistically quite similar to the surface charge models, the contamination barrier models do not offer a quantitative or mechanistic reason why the stable radius should be several hundred nanometers, and nor do they explain the sensitivity of the DLS-implied bubble radius to Debye length.

Although the charge stabilization appears to be the most complete or promising mechanism for the stability of bulk nanobubbles, experimental validation is a remote possibility. Ultimately, the charge stabilization model relies on an authoritative measurement of the zeta potential of the water-gas interface. This turns out to be a formidable task. Modern zeta potentiometry of nanoscale objects is predominantly based on light scattering, and therefore suffers from the significant issues with reproducibility mentioned earlier. These measurements do, however, consistently claim that objects believed to be bulk nanobubbles have a zeta potential in the region of -10 mV. A much less frequently used technique is optical zeta potentiometry, which enjoys the clear advantage of being able to probe the zeta potential of an individual object, but also the clear disadvantage of not being able to resolve anything below the optical resolution limit (typically a few microns). The measurements of Takahashi *et al.* [81] tantalizingly show that a shrinking  $\sim 10$   $\mu$ m microbubble (that can be verified to be of gaseous origin) will *diverge* from the planar zeta potential of -30 mV to about -60 mV before it becomes too small to be optically resolvable. It is not clear which of these perspectives is the correct one, and as a result the models are forced to make a choice. The model of Tan, An and Ohl [65] is developed around the optical zeta potentiometry experiments of Takahashi, Chiba and Li [81], while Zhang, Guo and Zhang [66] develop theirs around measurements around the much broader body of results on light scattering zeta potentiometry.

An even more intractable problem with proving the validity of the charge stabilization model lies with the ambiguity over what these experiments are actually measuring in the first place. Each zeta potentiometry technique estimates zeta potential by interrogating an unknown cross-section of the electric double layer. This ambiguity is not limited to experiments [82]. Whereas experiments at least agree about the sign and order of magnitude of the zeta potential, simulations nearly universally report that the water-air interface is positively charged, and *highly* acidic! Fortunately, the charge stabilization models do not necessarily require the net charge on the interface to be negative—the models work equally well

596 with a positive net charge—but the question of what the experiments are actually  
597 measuring remains frustratingly open.

## 598 **5. Outlook**

599 Significant strides have been made in the theoretical understanding of both  
600 surface and bulk nanobubbles in the last few years, yet there remain a number of  
601 interesting open problems worth pursuing.

### 602 *5.1. Experimental validation of theory*

603 Although the models presented in this paper comprehensively account for the  
604 main properties of both surface and bulk nanobubbles, the prospect of a compre-  
605 hensive experimental validation remains distant. With surface nanobubbles, the  
606 path towards full experimental validation of the TAO model will depend on the  
607 ability to experimentally resolve the potential between a gas molecule and an im-  
608 mersed substrate. Force microscopy techniques such as SFA or AFM measure the  
609 interaction between a probe and the immersed surface, as opposed to the interac-  
610 tion between a single molecule and an immersed surface that is required by the  
611 model.

612 In the case of bulk nanobubbles, we envisage that the surface charge model  
613 can be authoritatively proven or disproven by extending the *in situ* pressurization  
614 techniques pioneered by Alheshibri and Craig [60] to probe the compressibility of  
615 objects subjected to *tensile* stresses, and not just compressive ones. Although the  
616 lack of response of objects claimed to be bulk nanobubbles to compressive stresses  
617 is theoretically expected, a finding that they are also resilient to tensile stresses  
618 would re-open the theoretical debate in this field. The experiments of Jin *et al.* [79]  
619 offers the most promising path to proving the existence of bulk nanobubbles, as  
620 it allows one to track the shrinkage of microbubbles (whose gaseous origin can  
621 be easily and unambiguously ascertained) and ascertain their presence even when  
622 they are too small to be distinguished by standard brightfield microscopy.

### 623 *5.2. Solvent exchange*

624 One of the most intriguing subplots of the surface nanobubble story concerns  
625 the matter of producing them. About 20 years ago, it was accidentally discovered  
626 by Lou *et al.* [83] that surface nanobubbles nucleate on a surface that is initially  
627 wetted with an organic solvent of high gas solubility, before the liquid is replaced

with water, which has a much lower solubility. The phenomenon of *solvent exchange* is remarkably simple and efficacious compared to techniques such as nanodispensing, but the mechanistic principles behind its ability to nucleate nanobubbles are poorly understood. A beautifully designed MD study by Xiao *et al.* [84] that attempts to simulate solvent exchange reveals a remarkable paradox: when a poor solvent of gas dissolves a good one, dissolved gas is advected *towards* the substrate and against its putative concentration gradient! Then, the dissolved gas assembles at large concentrations adjacent to the substrate, triggering nucleation by driving down the nucleation energy barrier [85].

### 5.3. *Molecular dynamics simulations*

The inability of MD simulations to simulate realistically gas-saturated liquids (Section 3.6), means that we urge caution when using MD simulations to draw quantitative inferences about how surface nanobubbles behave under experimental conditions. Nevertheless, due to their ability to probe length and time scales inaccessible by experiment, MD studies have and will continue to provide illuminating qualitative insights about nanobubbles and other fluid dynamical or transport processes at the nanoscale. A non-exhaustive list of recent insights include nucleation by solvent exchange [84], pinning and force balance at the contact line [51, 86], and an impressive computational validation of the salient ideas of the pinning-oversaturation model [50].

We expect that MD simulations of realistically gas-saturated liquid will become feasible in future. The most obvious path to feasibility is that further improvements to computational power that allow million-atom simulations to become commonplace, facilitating explicit simulation of 10 ppm liquids. A more technically sophisticated path would lie in the development of coarse graining or hybrid molecular-continuum techniques [87, 88] that would allow systems such as nanobubbles to be investigated with vastly reduced computational resources. Among the complications in simulating weak solutions, however, is the need to handle chemical potential shifts (particularly of the dissolved gas solute) under a coarse-graining operation.

### 5.4. *The thermodynamics of nanobubbles*

Given the longevity of nanobubbles and their ability to reach a stable dynamic equilibrium, the tempting conclusion is that nanobubbles are in a state of thermodynamic equilibrium. It has however proven somewhat difficult to establish this authoritatively in a thermodynamic framework. Unfortunately, the typical approach is to take the approximation that atmospheric gases have no contribution

664 to the system's free energy, and therefore regard a nanobubble as a vapour bubble.  
665 An early paper [89] taking this approach was sharply criticised by Seddon and  
666 Zandvliet [90] because surface nanobubbles predominantly contain atmospheric  
667 gases, which would behave dramatically differently from pure vapour bubbles, but  
668 the criticisms equally apply to several other papers as well.

669 The best attempt to account for the presence of dissolved gas within a thermo-  
670 dynamic theory of surface nanobubbles comes from Zargarzadeh and Elliott [85],  
671 which in turn builds on seminal papers by C. A. Ward and colleagues [91]. It  
672 is our view that intriguing questions concerning the interplay of thermodynamics  
673 and wettability of surface nanobubbles, such as the breakdown of contact angle  
674 reciprocity between nanobubbles and nanodroplets [92], will require atmospheric  
675 gases to be explicitly treated.

## 676 **Acknowledgement**

677 H.A. acknowledges the support from the Australian Research Council Future  
678 Fellowship (FT180100361). C.D.O. acknowledges support through a joint re-  
679 search program between the Natural Science Foundation of China (Program No.  
680 11861131005) and the Deutsche Forschungsgemeinschaft of Germany (Program  
681 No. OH 75/3-1) and the European Social Fund (No. ZS/2019/10/103050) as part  
682 of the initiative "Sachsen-Anhalt WISSENSCHAFT Spitzenforschung/Synergien".

## 683 **Appendix A. Highlighted papers**

### 684 *Appendix A.1. Of outstanding interest*

- 685 • Brenner and Lohse [21]: The first paper to implicate substrate hydropho-  
686 bicity in the stability of surface nanobubbles.
- 687 • Tortora *et al.* [36]: Provides mechanistic explanations for stability or insta-  
688 bility of surface nanobubbles on hydrophilic surfaces and organic solvents.
- 689 • Tan, An and Ohl [35]: Reconciles three distinct perspectives of surface  
690 nanobubbles [21, 27, 31] into a single framework.
- 691 • Lohse and Zhang [31]: The first paper to mechanistically explain how sur-  
692 face nanobubbles can achieve stable equilibrium.

693 *Appendix A.2. Of special interest*

- 694 • Maheshwari *et al.* [50]: Molecular dynamics simulations that numerically  
695 and qualitatively confirm the key ideas of the pinning-oversaturation model,  
696 such as stability of contact line pinned surface nanobubbles to dissolution.
  - 697 • Xiao *et al.* [84]: A beautifully designed simulation study qualitatively re-  
698 solving gas transport processes during solvent exchange.
  - 699 • Zhang, Guo and Zhang [66]: A theory for stability of bulk nanobubbles  
700 building on the Akulichev model of charge stabilization that also takes am-  
701 bient liquid oversaturation into account.
  - 702 • Weijs and Lohse [27]: Explained the remarkably slow response of surface  
703 nanobubbles to environmental stimuli.
  - 704 • Zargarzadeh and Elliott [85]: Describes the stability of surface nanobubbles  
705 from a thermodynamic perspective; this is one of the few papers of its kind  
706 to correctly handle the presence of dissolved gas in the liquid.
  - 707 • Liu and Zhang [29]: The first to propose that surface nanobubbles can be  
708 stabilized by gas oversaturation and contact line pinning.
- 709 [1] W. Lauterborn, C.-D. Ohl, Cavitation bubble dynamics, Ultrasonics sono-  
710 chemistry 4 (1997) 65–75.
- 711 [2] C.-Y. Lai, J. Eggers, L. Deike, Bubble bursting: Universal cavity and jet  
712 profiles, Physical review letters 121 (2018) 144501.
- 713 [3] M. Alheshibri, J. Qian, M. Jehannin, V. S. Craig, A history of nanobubbles,  
714 Langmuir 32 (2016) 11086–11100.
- 715 [4] A. Martin, Japanese Firms Bet on Bub-  
716 ble Economy, Wall Street Journal (2016). URL:  
717 <https://www.wsj.com/articles/japanese-firms-bet-on-bubble-economy-1456670529>.
- 718 [5] J. L. Parker, P. M. Claesson, P. Attard, Bubbles, cavities, and the long-  
719 ranged attraction between hydrophobic surfaces., The Journal of Physical  
720 Chemistry 98 (1994) 8468–8480.
- 721 [6] H. Teshima, K. Takahashi, Y. Takata, T. Nishiyama, Wettability of afm tip  
722 influences the profile of interfacial nanobubbles, Journal of Applied Physics  
723 123 (2018) 054303.



- 724 [7] J. Crank, The mathematics of diffusion, Oxford university press, 1979.
- 725 [8] P. S. Epstein, M. S. Plesset, On the stability of gas bubbles in liquid-gas  
726 solutions, The Journal of Chemical Physics 18 (1950) 1505–1509.
- 727 [9] P. B. Duncan, D. Needham, Test of the epstein- plesset model for gas mi-  
728 croparticle dissolution in aqueous media: effect of surface tension and gas  
729 undersaturation in solution, Langmuir 20 (2004) 2567–2578.
- 730 [10] L. I. Berge, Dissolution of air bubbles by the resistive pulse and the pressure  
731 reversal technique, Journal of colloid and interface science 134 (1990) 548–  
732 562.
- 733 [11] E. E. Meyer, K. J. Rosenberg, J. Israelachvili, Recent progress in under-  
734 standing hydrophobic interactions, Proceedings of the National Academy of  
735 Sciences 103 (2006) 15739–15746.
- 736 [12] A. Poynor, L. Hong, I. K. Robinson, S. Granick, Z. Zhang, P. A. Fenter,  
737 How water meets a hydrophobic surface, Physical review letters 97 (2006)  
738 266101.
- 739 [13] M. Mezger, H. Reichert, S. Schöder, J. Okasinski, H. Schröder, H. Dosch,  
740 D. Palms, J. Ralston, V. Honkimäki, High-resolution in situ x-ray study of  
741 the hydrophobic gap at the water–octadecyl-trichlorosilane interface, Pro-  
742 ceedings of the National Academy of Sciences 103 (2006) 18401–18404.
- 743 [14] X. H. Zhang, G. Li, N. Maeda, J. Hu, Removal of induced nanobubbles  
744 from water/graphite interfaces by partial degassing, Langmuir 22 (2006)  
745 9238–9243.
- 746 [15] X. Zhang, D. Y. Chan, D. Wang, N. Maeda, Stability of interfacial nanobub-  
747 bles, Langmuir 29 (2013) 1017–1023.
- 748 [16] C.-W. Yang, Y.-H. Lu, S. Hwang, Imaging surface nanobubbles at graphite–  
749 water interfaces with different atomic force microscopy modes, Journal of  
750 Physics: Condensed Matter 25 (2013) 184010.
- 751 [17] C. Xu, S. Peng, G. G. Qiao, V. Gutowski, D. Lohse, X. Zhang, Nanobubble  
752 formation on a warmer substrate, Soft Matter 10 (2014) 7857–7864.

- 753 [18] C. U. Chan, C.-D. Ohl, Total-internal-reflection-fluorescence microscopy  
754 for the study of nanobubble dynamics, *Physical review letters* 109 (2012)  
755 174501.
- 756 [19] X. Zhang, Z. Wu, X. Zhang, G. Li, J. Hu, Nanobubbles at the interface of  
757 hopg and ethanol solution, *International Journal of Nanoscience* 4 (2005)  
758 399–407.
- 759 [20] J. Qian, V. S. Craig, M. Jehannin, Long-term stability of surface nanobubbles  
760 in undersaturated aqueous solution, *Langmuir* 35 (2018) 718–728.
- 761 [21] M. P. Brenner, D. Lohse, Dynamic equilibrium mechanism for surface  
762 nanobubble stabilization, *Physical review letters* 101 (2008) 214505.
- 763 [22] J. R. Seddon, H. J. Zandvliet, D. Lohse, Knudsen gas provides nanobubble  
764 stability, *Physical review letters* 107 (2011) 116101.
- 765 [23] E. Dietrich, H. J. Zandvliet, D. Lohse, J. R. Seddon, Particle tracking around  
766 surface nanobubbles, *Journal of physics: Condensed matter* 25 (2013)  
767 184009.
- 768 [24] W. A. Ducker, Contact angle and stability of interfacial nanobubbles, *Lang-*  
769 *muir* 25 (2009) 8907–8910.
- 770 [25] S. R. German, X. Wu, H. An, V. S. Craig, T. L. Mega, X. Zhang, Interfacial  
771 nanobubbles are leaky: Permeability of the gas/water interface, *ACS nano* 8  
772 (2014) 6193–6201.
- 773 [26] S. M. Dammer, D. Lohse, Gas enrichment at liquid-wall interfaces, *Physical*  
774 *review letters* 96 (2006) 206101.
- 775 [27] J. H. Weijs, D. Lohse, Why surface nanobubbles live for hours, *Physical*  
776 *review letters* 110 (2013) 054501.
- 777 [28] Y. Liu, X. Zhang, Nanobubble stability induced by contact line pinning, *The*  
778 *Journal of chemical physics* 138 (2013) 014706.
- 779 [29] Y. Liu, X. Zhang, A unified mechanism for the stability of surface nanobub-  
780 bles: Contact line pinning and supersaturation, *The Journal of Chemical*  
781 *Physics* 141 (2014) 134702.

- 782 [30] Y. Liu, J. Wang, X. Zhang, W. Wang, Contact line pinning and the relation-  
783 ship between nanobubbles and substrates, *The Journal of Chemical Physics*  
784 140 (2014) 054705.
- 785 [31] D. Lohse, X. Zhang, et al., Pinning and gas oversaturation imply stable  
786 single surface nanobubbles, *Physical Review E* 91 (2015) 031003.
- 787 [32] C. U. Chan, M. Arora, C.-D. Ohl, Coalescence, growth, and stability of  
788 surface-attached nanobubbles, *Langmuir* 31 (2015) 7041–7046.
- 789 [33] H. An, B. H. Tan, Q. Zeng, C.-D. Ohl, Stability of nanobubbles formed at  
790 the interface between cold water and hot highly oriented pyrolytic graphite,  
791 *Langmuir* 32 (2016) 11212–11220.
- 792 [34] B. H. Tan, H. An, C.-D. Ohl, et al., Surface nanobubbles are stabilized by  
793 hydrophobic attraction, *Physical review letters* 120 (2018) 164502.
- 794 [35] B. H. Tan, H. An, C.-D. Ohl, Stability, dynamics, and tolerance to undersat-  
795 uration of surface nanobubbles, *Physical review letters* 122 (2019) 134502.
- 796 [36] M. Tortora, S. Meloni, B. H. Tan, A. Giacomello, C.-D. Ohl, C. M. Casci-  
797 ola, The interplay among gas, liquid and solid interactions determines the  
798 stability of surface nanobubbles, *Nanoscale* (2020).
- 799 [37] H. An, B. H. Tan, C.-D. Ohl, Distinguishing nanobubbles from nanodroplets  
800 with afm: the influence of vertical and lateral imaging forces, *Langmuir* 32  
801 (2016) 12710–12715.
- 802 [38] N. D. Petsev, L. G. Leal, M. S. Shell, Universal gas adsorption mecha-  
803 nism for flat nanobubble morphologies, *Physical Review Letters* 125 (2020)  
804 146101.
- 805 [39] H. Swenson, N. P. Stadie, Langmuir’s theory of adsorption: A centennial  
806 review, *Langmuir* 35 (2019) 5409–5426.
- 807 [40] S. Maheshwari, M. van der Hoef, J. Rodriguez Rodriguez, D. Lohse, Leak-  
808 iness of pinned neighboring surface nanobubbles induced by strong gas–  
809 surface interaction, *ACS nano* 12 (2018) 2603–2609.
- 810 [41] B. Dollet, D. Lohse, Pinning stabilizes neighboring surface nanobubbles  
811 against ostwald ripening, *Langmuir* 32 (2016) 11335–11339.

- 812 [42] L. Zhou, X. Wang, H.-J. Shin, J. Wang, R. Tai, X. Zhang, H. Fang, W. Xiao,  
813 L. Wang, C. Wang, et al., Ultrahigh density of gas molecules confined in  
814 surface nanobubbles in ambient water, *Journal of the American Chemical*  
815 *Society* 142 (2020) 5583–5593.
- 816 [43] C.-L. Wang, Z.-X. Li, J.-Y. Li, P. Xiu, J. Hu, H.-P. Fang, High density gas  
817 state at water/graphite interface studied by molecular dynamics simulation,  
818 *Chinese Physics B* 17 (2008) 2646.
- 819 [44] L. Zhang, H. Chen, Z. Li, H. Fang, J. Hu, Long lifetime of nanobubbles due  
820 to high inner density, *Science in China Series G: Physics, Mechanics and*  
821 *Astronomy* 51 (2008) 219–224.
- 822 [45] H.-P. Fang, J. Hu, Molecular dynamics simulation studies on some topics of  
823 water molecules on hydrophobic surfaces, *Nuclear Science and Techniques*  
824 17 (2006) 71–77.
- 825 [46] S. Wang, L. Zhou, X. Wang, C. Wang, Y. Dong, Y. Zhang, Y. Gao, L. Zhang,  
826 J. Hu, Force spectroscopy revealed a high-gas-density state near the graphite  
827 substrate inside surface nanobubbles, *Langmuir* 35 (2019) 2498–2505.
- 828 [47] R. Battino, H. L. Clever, The solubility of gases in liquids, *Chemical Re-*  
829 *views* 66 (1966) 395–463.
- 830 [48] L. Wang, X. Wang, L. Wang, J. Hu, C. L. Wang, B. Zhao, X. Zhang, R. Tai,  
831 M. He, L. Chen, et al., Formation of surface nanobubbles on nanostructured  
832 substrates, *Nanoscale* 9 (2017) 1078–1086.
- 833 [49] D. S. Bull, N. Nelson, D. Konetski, C. N. Bowman, D. K. Schwartz, A. P.  
834 Goodwin, Contact line pinning is not required for nanobubble stability on  
835 copolymer brushes, *The journal of physical chemistry letters* 9 (2018) 4239–  
836 4244.
- 837 [50] S. Maheshwari, M. van der Hoef, X. Zhang, D. Lohse, Stability of surface  
838 nanobubbles: A molecular dynamics study, *Langmuir* 32 (2016) 11116–  
839 11122.
- 840 [51] J. Fan, J. De Coninck, H. Wu, F. Wang, Microscopic origin of capillary force  
841 balance at contact line, *Physical Review Letters* 124 (2020) 125502.

- 842 [52] M. C. Lopes, E. Bonaccorso, Evaporation control of sessile water drops by  
843 soft viscoelastic surfaces, *Soft Matter* 8 (2012) 7875–7881.
- 844 [53] J. Gerber, T. Lendenmann, H. Eghlidi, T. M. Schutzius, D. Poulikakos, Wet-  
845 ting transitions in droplet drying on soft materials, *Nature communications*  
846 10 (2019) 1–10.
- 847 [54] R. W. Style, A. Jagota, C.-Y. Hui, E. R. Dufresne, Elastocapillarity: Surface  
848 tension and the mechanics of soft solids, *Annual Review of Condensed*  
849 *Matter Physics* 8 (2017) 99–118.
- 850 [55] K. A. Mørch, Reflections on cavitation nuclei in water, *Physics of Fluids* 19  
851 (2007) 072104.
- 852 [56] A. Häbich, W. Ducker, D. E. Dunstan, X. Zhang, Do stable nanobubbles  
853 exist in mixtures of organic solvents and water?, *The Journal of Physical*  
854 *Chemistry B* 114 (2010) 6962–6967.
- 855 [57] F. Eklund, J. Swenson, Stable air nanobubbles in water: the importance of  
856 organic contaminants, *Langmuir* 34 (2018) 11003–11009.
- 857 [58] A. J. Jadhav, M. Barigou, Bulk nanobubbles or not nanobubbles: That is the  
858 question, *Langmuir* 36 (2020) 1699–1708.
- 859 [59] A. J. Jadhav, M. Barigou, Proving and interpreting the spontaneous forma-  
860 tion of bulk nanobubbles in aqueous organic solvent solutions: effects of  
861 solvent type and content, *Soft Matter* 16 (2020) 4502–4511.
- 862 [60] M. Alheshibri, V. S. Craig, Differentiating between nanoparticles and  
863 nanobubbles by evaluation of the compressibility and density of nanopar-  
864 ticles, *The Journal of Physical Chemistry C* 122 (2018) 21998–22007.
- 865 [61] M. Alheshibri, V. S. Craig, Armoured nanobubbles; ultrasound contrast  
866 agents under pressure, *Journal of colloid and interface science* 537 (2019)  
867 123–131.
- 868 [62] M. Alheshibri, V. S. Craig, Generation of nanoparticles upon mixing ethanol  
869 and water; nanobubbles or not?, *Journal of colloid and interface science* 542  
870 (2019) 136–143.
- 871 [63] V. Akulichev, Hydration of ions and the vacitation resistance of water,  
872 *Acoustical Physics* 12 (1966) 144–150.

- 873 [64] K. Yasui, T. Tuziuti, W. Kanematsu, K. Kato, Dynamic equilibrium model  
874 for a bulk nanobubble and a microbubble partly covered with hydrophobic  
875 material, *Langmuir* 32 (2016) 11101–11110.
- 876 [65] B. H. Tan, H. An, C.-D. Ohl, How bulk nanobubbles might survive, *Physical*  
877 *Review Letters* 124 (2020) 134503.
- 878 [66] H. Zhang, Z. Guo, X. Zhang, Surface enrichment of ions leads to stability  
879 of bulk nanobubbles, *Soft Matter* (2020).
- 880 [67] G. Quincke, Ueber die fortführung materieller theilchen durch strömende  
881 elektricität, *Annalen der Physik* 189 (1861) 513–598.
- 882 [68] H. McTaggart, Xxxiii. the electrification at liquid-gas surfaces, *The London,*  
883 *Edinburgh, and Dublin Philosophical Magazine and Journal of Science* 27  
884 (1914) 297–314.
- 885 [69] N. Bunkin, F. Bunkin, Bubbstons: stable microscopic gas bubbles in very  
886 dilute electrolytic solutions (1992).
- 887 [70] H. Ohshima, T. W. Healy, L. R. White, Accurate analytic expressions for the  
888 surface charge density/surface potential relationship and double-layer po-  
889 tential distribution for a spherical colloidal particle, *Journal of colloid and*  
890 *interface science* 90 (1982) 17–26.
- 891 [71] K. Ebina, K. Shi, M. Hirao, J. Hashimoto, Y. Kawato, S. Kaneshiro, T. Mori-  
892 moto, K. Koizumi, H. Yoshikawa, Oxygen and air nanobubble water solution  
893 promote the growth of plants, fishes, and mice, *PLoS One* 8 (2013) e65339.
- 894 [72] E. Stride, N. Saffari, Microbubble ultrasound contrast agents: a review,  
895 *Proceedings of the Institution of Mechanical Engineers, Part H: Journal of*  
896 *Engineering in Medicine* 217 (2003) 429–447.
- 897 [73] N. Taccoen, F. Lequeux, D. Z. Gunes, C. N. Baroud, Probing the mechan-  
898 ical strength of an armored bubble and its implication to particle-stabilized  
899 foams, *Physical Review X* 6 (2016) 011010.
- 900 [74] G. S. Manning, On the thermodynamic stability of bubbles, immiscible  
901 droplets, and cavities, *Physical Chemistry Chemical Physics* 22 (2020)  
902 17523–17531.

- 903 [75] S. Kim, D. Kim, J. Kim, S. An, W. Jhe, Direct evidence for curvature-  
904 dependent surface tension in capillary condensation: Kelvin equation at  
905 molecular scale, *Physical Review X* 8 (2018) 041046.
- 906 [76] A. E. van Giessen, E. M. Blokhuis, Direct determination of the tolman length  
907 from the bulk pressures of liquid drops via molecular dynamics simulations,  
908 *The Journal of chemical physics* 131 (2009) 164705.
- 909 [77] Q. Kim, W. Jhe, Interfacial thermodynamics of spherical nanodroplets:  
910 Molecular understanding of surface tension via hydrogen bond network,  
911 *arXiv preprint arXiv:2004.12533* (2020).
- 912 [78] H. Y. Lo, Y. Liu, S. Y. Mak, Z. Xu, Y. Chao, K. J. Li, H. C. Shum, L. Xu,  
913 Diffusion-dominated pinch-off of ultralow surface tension fluids, *Physical*  
914 *review letters* 123 (2019) 134501.
- 915 [79] J. Jin, R. Wang, J. Tang, L. Yang, Z. Feng, C. Xu, F. Yang, N. Gu, Dynamic  
916 tracking of bulk nanobubbles from microbubbles shrinkage to collapse, *Col-*  
917 *loids and Surfaces A: Physicochemical and Engineering Aspects* 589 (2020)  
918 124430.
- 919 [80] K. Ohgaki, N. Q. Khanh, Y. Joden, A. Tsuji, T. Nakagawa, Physicochemical  
920 approach to nanobubble solutions, *Chemical Engineering Science* 65 (2010)  
921 1296–1300.
- 922 [81] M. Takahashi, K. Chiba, P. Li, Free-radical generation from collapsing mi-  
923 crobubbles in the absence of a dynamic stimulus, *The Journal of Physical*  
924 *Chemistry B* 111 (2007) 1343–1347.
- 925 [82] R. J. Saykally, Two sides of the acid–base story, *Nature chemistry* 5 (2013)  
926 82–84.
- 927 [83] S.-T. Lou, Z.-Q. Ouyang, Y. Zhang, X.-J. Li, J. Hu, M.-Q. Li, F.-J. Yang,  
928 Nanobubbles on solid surface imaged by atomic force microscopy, *Jour-*  
929 *nal of Vacuum Science & Technology B: Microelectronics and Nanometer*  
930 *Structures Processing, Measurement, and Phenomena* 18 (2000) 2573–2575.
- 931 [84] Q. Xiao, Y. Liu, Z. Guo, Z. Liu, D. Lohse, X. Zhang, Solvent exchange  
932 leading to nanobubble nucleation: A molecular dynamics study, *Langmuir*  
933 33 (2017) 8090–8096.

- 934 [85] L. Zargarzadeh, J. A. Elliott, Thermodynamics of surface nanobubbles,  
935 Langmuir 32 (2016) 11309–11320.
- 936 [86] J.-C. Fernandez-Toledano, C. Rigaut, M. Mastrangeli, J. De Coninck, Con-  
937 trolling the pinning time of a receding contact line under forced wetting con-  
938 ditions, Journal of colloid and interface science 565 (2020) 449–457.
- 939 [87] N. D. Petsev, L. G. Leal, M. S. Shell, Hybrid molecular-continuum simula-  
940 tions using smoothed dissipative particle dynamics, The Journal of Chemical  
941 Physics 142 (2015) 044101.
- 942 [88] N. D. Petsev, L. G. Leal, M. S. Shell, Multiscale simulation of ideal mix-  
943 tures using smoothed dissipative particle dynamics, The Journal of Chemical  
944 Physics 144 (2016) 084115.
- 945 [89] R. Colaço, A. Serro, B. Saramago, On the stability of bubbles trapped at  
946 a solid–liquid interface: a thermodynamical approach, Surface science 603  
947 (2009) 2870–2873.
- 948 [90] J. R. Seddon, H. J. Zandvliet, Comment on:“on the stability of bubbles  
949 trapped at a solid–liquid interface: A thermodynamical approach”, Surface  
950 Science 3 (2010) 476–477.
- 951 [91] C. A. Ward, A. Balakrishnan, F. C. Hooper, On the thermodynamics of  
952 nucleation in weak gas-liquid solutions (1970).
- 953 [92] H. Zhang, X. Zhang, Size dependence of bubble wetting on surfaces: break-  
954 down of contact angle match between small sized bubbles and droplets,  
955 Nanoscale 11 (2019) 2823–2828.